NASA Technical Memorandum 80053

NASA-TM-80053 19790010515

APPLICATIONS OF DIFFRACTION THEORY TO AEROACOUSTICS

DONALD L. LANSING
CHEN-HUEI LIU
THOMAS D. NORUM

JANUARY 1979

National Aeronautics and
Space Administration

Langley Research Center
Hampton, Virginia 23665

1 Report No	2 Government Accession No	3 Recipient's Catalog No
TM 80053		

4 Title and Subtitle	5 Report Date
Applications of Diffraction Theory to Aeroacoustics	January 1979
	6 Performing Organization Code
7 Author(s)	8 Performing Organization Report No
Donald L. Lansing, Chen-Huei Liu, and Thomas D. Norum	
9 Performing Organization Name and Address	10 Work Unit No
NASA Langley Research Center Hampton, Virginia 23555	505-03-13-17
	11 Contract or Grant No
	13 Type of Report and Period Covered
12 Sponsoring Agency Name and Address	Technical Memorandum
National Aeronautics and Space Administration Washington, DC 20546	14 Sponsoring Agency Code

15 Supplementary Notes

To be presented as a paper and included in the proceedings of the VKI/AGARD Special Course to be held in Brussels, Belgium, May 28-June 1, 1979.

16 Abstract

This paper reviews the fundamentals of diffraction theory and the application of the theory to several problems of aircraft noise generation, propagation, and measurement. The general acoustic diffraction problem is defined and the governing equations set down. Diffraction phenomena are illustrated using the classical problem of the diffraction of a plane wave by a half-plane. Infinite series and geometric acoustic methods for solving diffraction problems are described. Four applications of diffraction theory are discussed: the selection of an appropriate shape for a microphone, the use of aircraft wings to shield the community from engine noise, the reflection of engine noise from an aircraft fuselage and the radiation of trailing edge noise.

17 Key Words (Suggested by Author(s))	18 Distribution Statement
Aeroacoustics Wave Propagation Scattering	Unclassified - Unlimited Subject Category 71

19 Security Classif (of this report)	20 Security Classif (of this page)	21 No of Pages	22 Price*
Unclassified	Unclassified	12	$4.00

* For sale by the National Technical Information Service Springfield Virginia 22161

APPLICATIONS OF DIFFRACTION THEORY TO AEROACOUSTICS

Donald L. Lansing
Head, Aeroacoustics Branch
Chen-Huei Liu
Aero-Space Technologist
Thomas D. Norum
Aero-Space Technologist
NASA Langley Research Center
Hampton, Virginia 23365

SUMMARY

This paper reviews the fundamentals of diffraction theory and the application of the theory to several problems of aircraft noise generation, propagation, and measurement The general acoustic diffraction problem is defined and the governing equations set down Diffraction phenomena are illustrated using the classical problem of the diffraction of a plane wave by a half-plane Infinite series and geometric acoustic methods for solving diffraction problems are described Four applications of diffraction theory are discussed the selection of an appropriate shape for a microphone, the use of aircraft wings to shield the community from engine noise, the reflection of engine noise from an aircraft fuselage and the radiation of trailing edge noise

INTRODUCTION

There is a growing appreciation for the role of diffraction phenomena in aircraft noise research Diffraction occurs for example in the propagation and radiation of engine noise from internal ducts, the scattering of engine noise from aircraft wing, fuselage and tail surfaces, and the design and calibration of special sensors for acoustic measurements. While diffraction theory is a branch of classical mathematical physics with a voluminous literature, most available results are for pure tone plane wave, line, or point sources diffracted by simple shapes Aeroacousticians are presented with severe challenges in extending this body of work to broadband, distributed noise sources and complex aircraft geometry in the presence of a turbulent moving medium

This paper is a blend of textbook results on diffraction theory and some current problems in noise generation and measurement The literature on diffraction is vast Excellent bibliographies and comprehensive introductions to the theory can be found in references 1, 2, and 3 To lay a foundation for understanding the later examples the paper begins by reviewing the essentials of diffraction theory The governing equations are set out, the important physical phenomena are reviewed, and two solution methods used in the practical applications are described Four applications of diffraction theory to aircraft noise related problems are discussed selection of an appropriate shape for a pressure gradient microphone, the reduction of community noise through wing shielding effects, the reflection of engine noise from aircraft fuselage surfaces, and the radiation of trailing edge noise The paper provides useful background information for the lecture by L Maestrello and A Bayliss in this series entitled "Acoustic Scattering from an Elliptical Body "

BASIC EQUATIONS OF ACOUSTIC DIFFRACTION THEORY

A sketch of the general acoustic diffraction problem and the field equations and auxiliary conditions of diffraction theory are shown in Figures 1 and 2, references 2 and 3 An incident sound field from either an incoming wave or a source distribution Q impinges upon a body Due to the presence of the body a secondary or scattered field is produced The complete wave field is a superposition of the incident and scattered fields The basic mathematical problem is to predict the scattered and total acoustic wave fields

The inhomogeneous wave equation is the partial differential equation which governs the incident and scattered sound fields The source distribution Q, when it occurs, appears on the right hand side of this equation The physically measurable quantities in the sound field, that is, the acoustic pressure P and the acoustic velocity vector $\underline{u}$, are determined from the velocity potential ϕ by taking the time derivative and gradient respectively as indicated at the bottom of Figure 1 For a solution of the field equations to be acceptable from a physical viewpoint, the pressure and velocity must be continuous throughout the wave field

In addition to satisfying the inhomogeneous wave equation, the solution must also satisfy several auxiliary conditions listed in Figure 2 The first of these is the surface boundary condition which states that the ratio of the normal acoustic velocity to the pressure at any point on the surface must equal the prescribed surface admittance ν On a hard surface $\nu = 0$ Nonzero and generally complex values of ν designate various degrees of absorption and compliance for nonrigid surfaces

The second condition called the radiation condition, assures that, with the exception of a prescribed incident wave, the solution consists only of outgoing waves at large distances from the body That is, in the acoustic far field the additional disturbance produced by the presence of the scattering object must appear to originate at the object and produce waves which propagate away from it Another way to state the radiation condition is that the pressure and radial component of acoustic velocity must be in phase in the far field The third condition, the edge condition, is required to ensure the uniqueness of solutions for problems in which the scattering body has very sharp edges as when, for example, the body is a thin screen or disc of zero thickness From a physical point of view the edge condition assures that no sound energy is generated at a sharp edge

PLANE WAVE DIFFRACTION BY A HALF PLANE

Considerable insight into diffraction phenomena can be had by considering the problem of the diffraction of a plane acoustic wave by a very large flat surface idealized as a semi-infinite half plane A two-dimensional formulation of this problem is shown in Figure 3 The half plane or screen is perfectly rigid so that the normal component of the acoustic velocity on the screen is zero

Consider, first of all, a description of the sound field from the standpoint of geometric acoustics in which it is assumed that sound travels along straight rays Then the sound field may be decomposed into three principle regions Region I, called the geometric shadow, receives none of the incident sound and is completely silent The sonified region, that is, the region in which sound can be received along straight rays from the source, consistsof two subregions Within region II sound is received only from the incident plane wave Region III, however, receives not only direct radiation from the incident plane wave but also sound which is reflected from the lower half of the screen

This description is mathematically discontinuous across both the shadow boundary and the reflected edge ray Thus, the geometric acoustic solution exhibits discrete jumps which are unacceptable physically and theoretically The complete solution requires an additional wave field called the "diffracted wave" which provides a smooth transition between all of the regions and makes for a solution which is continuous everywhere The table at the bottom of Figure 3 summarizes the wave constituents in these three regions

The exact mathematical solution of this diffraction problem is shown in Figure 4, see references 2 and 4 The origin of the polar coordinates (r, θ) of the observer is at the edge of the half plane $k = \omega/c$ is the wave number of the incident wave in which ω is the angular frequency and c is the speed of sound The mathematical expression is a solution of the wave equation whose normal derivative vanishes at the surface of the half plane and which represents the prescribed incident plane wave The function $\Phi(x)$ is called a Fresnel integral These functions appear in many diffraction problems involving sharp edges Because of their frequent occurrance in wave propagation problems they have been extensively tabulated and computational subroutines have been devised for evaluating them accurately on high speed computing machines By replacing the Fresnel integrals by their approximations for very large values of kr one recovers precisely the geometric acoustic solution to this problem

A calculation of the mean square pressure in the sound field is shown in Figure 5 The calculation is for a normally incident sound wave as indicated in the sketch The calculation is made along an arc defined by $kr = 6\pi$ which corresponds to a radial distance equal to three times the wavelength of the incident sound The three regions described in Figure 3 are indicated at the top of the plot For reference it is useful to note the square of the pressure in the incident wave field is unity The intensity is very low but nonzero in the shadow region As one crosses the shadow boundary into the sonified region the intensity increases smoothly, overshoots the intensity in the incident wave, and then settles down after several oscillations to the incident wave value Well into region III the intensity is characterized by a number of large oscillations which are caused by the constructive and destructive interference between the incident wave and waves reflected from the screen The intensity maxima and minima occur at the same angles as though the half plane was infinitely large in both directions

SOLUTION METHODS FOR DIFFRACTION PROBLEMS

Obtaining a solution to the inhomogeneous wave equation which satisfies the appropriate auxiliary conditions for complex shapes and general source distributions over a wide range of frequencies is an extremely difficult problem for which there is no single comprehensive method Diffraction theory is a highly mathematical theory which is rich in subtle detail and great ingenuity Solution methods include for example the Kirchhoff approximation, integral equation formulations, function theoretic methods, series expansions, variational formulations, and ray theories In this paper two solution techniques will be briefly described which are suitable for fairly broad classes of diffraction problems The series method, which provides exact solutions for certain standard geometric shapes in the form of infinite series, and geometric theory, which gives an approximate solution for quite general shapes at high frequencies The details of these two methods will be illustrated for the diffraction of a plane wave by a rigid circular cylinder

Series Solution Method - Consider the two-dimensional problem of the diffraction of an incident plane wave by a rigid circular cylinder of radius a as indicated in Figure 6, reference 4 The velocity potential ϕ must be a solution of the homogeneous Helmholtz equation which represents an incoming plane wave and a system of outgoing scattered waves whose combination satisfies the boundary condition that the normal acoustic velocity at the surface of the cylinder vanishes A time factor $e^{-i\omega t}$ will be used in this paper

The velocity potential ϕ is represented as the sum of two potentials ϕ_1 corresponding to the incident plane wave and ϕ_S, the scattered potential, corresponding to the sum of all reflected and diffracted waves Choosing the plane wave to be incident on the cylinder from the negative x direction ϕ_1 takes the form shown in Figure 6 in which $\varepsilon_0 = 1$ and $\varepsilon_2 = \varepsilon_3 = \quad = 2$ An appropriate form for ϕ_S is given by the series at the bottom of the figure in which the A_n's are undetermined coefficients Each term in this infinite series is a solution of the wave equation which is finite and continuous everywhere outside of the cylinder and which represents sound waves radiating away from the cylinder The sum $\phi_1 + \phi_S$ satisfies all the conditions of the problem with the exception of the surface boundary condition on the cylinder

The complete expression for ϕ is shown in Figure 7 The unknown coefficients A_n are now determined by applying the boundary condition to this series expression This leads to the requirement that the Fourier series in θ be equal to zero which requires that each coefficient of the series be equal to zero The final equation for A_n is shown in the middle of Figure 7

By substituting these values for the A_n's back into the series expression for ϕ, one has the complete solution to the diffraction problem The acoustic pressures and velocities can be calculated at any point within the wave field by evaluating the appropriate infinite series expressions The infinite series is a

useful means for obtaining the numerical values of the solution for small values of ka but converges very slowly and requires many terms when ka is large, that is when the wavelength is much shorter than the cylinder radius In the acoustic far field the series for the scattered pressure can be approximated as shown at the bottom of Figure 7

Some calculations of the mean square pressure in the scattered wave obtained from this series are shown in Figure 8 The sketches are polar plots of $|P|^2$ for values of ka = 1, 3, and 5 These calculations were made using a maximum of 30 terms in the series which was found to be sufficient for values of ka as high as 10 The origin of each polar plot, indicated by the heavy black dot in the center of each sketch, corresponds to the center of the cylinder For values of ka less than 1, there is considerable backscatter from the cylinder in the direction of the incoming plane wave and relatively little sound scattered in the forward direction As ka increases, there is a tendency for the scattered wave to be beamed in the forward direction with a decrease, but a growing number of lobes, in the relative amplitude of the back scattered field

Geometric Theory - A wave theory solution requires solving the wave equation Numerous methods have been devised for finding wave solutions, but these methods generally only apply to simple geometries and are not always useful for practical applications Keller, reference 5, introduced the geometric theory of diffraction for solving approximately problems of wave propagation The method is intended to apply to high frequency waves, or, more precisely, to problems in which the wavelength λ is small compared to the dimensions of the scattering body In many practical cases it has been found that the method also gives useful results down to frequencies for which λ is comparable to scatter dimensions An important advantage of the geometrical theory is that it does not depend upon the separation of variables or any similar analytical procedure The shapes of objects to which it can be applied are quite general

The basic idea of the theory is that short acoustic waves propagate along straight rays as in geometrical optics However, the theory introduces new kinds of rays called "diffracted" rays In applying the geometric theory of diffraction the field at a point is calculated from the sum of fields from all the geometrical acoustics rays, i e , the direct and reflected rays, and all the diffracted rays The solution of the problem of the diffraction of a plane wave by a circular cylinder in two-dimension will now be derived using the geometric theory

First, it is necessary to calculate the wave field produced by the reflection of the incident plane wave from the cylinder, see Figure 9 The notation of the proceeding section of the paper is used Let $P_r(0)$ denote the reflected field at a point 0 One determines the amplitude A_r and the phase Φ of this wave as follows The amplitude of the reflected wave is determined by the conservation of energy along the incident and reflected rays at point 0' That is, the energy flux in the tube of rays incident upon and reflected from this point must be the same at all points along the tube The energy density along the tube is inversely proportional to the cross-sectional area of the tube, which can be determined from the Jacobian of the transformation between the physical variables (x,y) and the ray variables s and $\bar{\theta}$ The (x, y) phase Φ is assumed to be a linear function of the distance s along the reflected ray The constant s_0 is determined by requiring that the phase of the reflected pressure at 0' be identical to the phase of the incident pressure there The final expression for the reflected pressure is shown at the bottom of Figure 9 where it has been simplified for an observer in the acoustic far field In the geometric shadow $P_r(0) = 0$ since there are no reflected rays there

It is now necessary to calculate the diffracted field induced by the cylinder The result of this calculation is shown in Figure 10 Behind this calculation is significant extension of classical geometrical acoustics introduced by Keller who postulates that there exists a class of diffracted rays which account for the phenomena of diffraction These rays are produced when incident rays hit edges or corners of the scattering surface or when the incident ray impinges tangentially upon a smooth curved surface Some of the diffracted rays penetrate into the shadow regions and describe the diffracted field there Other rays modify the field in the sonified regions The value of the field on a diffracted ray is obtained by multiplying the field on the incident ray at the point of diffraction of a so called "diffraction coefficient " Diffraction coefficients are determined entirely by the local properties of the field and the boundary in the immediate neighborhood at the point of diffraction and hence may be determined from the solution of simple boundary value problems having these local properties

For the cylinder, diffracted rays emanate tangentially from all points of the cylinder surface These rays are produced by "creeping" waves or surface waves which appear to originate at points 0_1 and 0_2 on the upper and lower surface of the cylinder These waves encircle the cylinder in both directions and continuously radiate energy so that they steadily decay as they propagate The series for the diffracted pressure may be interpreted as the sum of infinitely many creeping waves The various orders of creeping waves are determined by the number of times the wave has encircled the cylinder The complete solution is therefore given by $P_1(0) + P_r(0) + P_d(0)$ which enables one to calculate the field at any point which does not lie on a caustic or a shadow boundary

The expression developed in Figures 9 and 10 will now be used to calculate the diffraction of a plane wave by a cylinder The amplitude of the field divided by the amplitude of the incident field is plotted along the x-axis for ka = 10 in Figure 11 The solid curve is computed using the series method from the preceding section of the paper The dot points are just the solution from the geometrical theory of diffraction (Noted that $P_r = 0$ in the forward direction) The comparison is seen to be quite acceptable

The remainder of this paper will consider four problems in applied acoustics in which diffraction phenomena play a central role The two solution methods just described have been used to obtain theoretical insight into these problems

DIFFRACTION BY PRESSURE GRADIENT MICROPHONES

A photograph of a pressure gradient microphone and a sketch indicating its operation are shown in Figure 12 The type of microphone shown in the photograph has the shape of a thick disc of diameter about 2 36 cm The purpose of this pressure sensor is to measure the pressure gradient in an incident wave field

as indicated in the sketch at the right The microphone consists of two pressure sensitive elements separated by a distance ΔZ The pressure gradient at the center of the microphone, 0, is then given approximately by the ratio $(P_T - P_B)/\Delta Z$ in which P_T and P_B are the pressures measured on the top and bottom sides of the microphone The actual pressures measured on the surfaces of the pressure gradient microphone will not be the desired free-field pressures because of diffraction effects The scattering factor σ defined at the bottom of the figure is a measure of the degree to which the measured pressure difference divided by the microphone thickness approximates the true free-field pressure gradient and is therefore a figure of merit for the operation of a pressure gradient microphone An analytical and experimental investigation was undertaken in order to determine an optimal shape which would minimize diffraction effects

In order to assess the effects of microphone shape upon the measured surface pressures and thereby determine shapes which introduce minimum distortion one needs a validated analytical procedure for predicting the surface pressures on a variety of microphone shapes The shape of the pressure gradient microphone in Figure 12 can be approximated as an oblate spheroid The wave equation is separable in oblate spheroidal coordinates and the diffraction of plane waves by such a spheroid can be solved using the series method described earlier in this paper, reference 6 Some coordinate lines for oblate spheroidal coordinates (ξ, η) are shown in Figure 13 The curves ξ = constant are ellipses which generate oblate spheroids when rotated about the Z axis The curves η = constant are hyperbolas Compared to polar coordinates, the coordinate ξ varies from the surface of the spheroid into the acoustic far field analogous to the radial coordinate r whereas η varies around the spheroid analogous to the angular coordinate θ As a matter of reference the coordinate η decreases from +1 on the positive Z axis to 0 in the mid-plane of the spheroid to -1 on the negative Z axis

The equation for calculating surface pressures at any point η on the surface of an oblate spheroid $\xi = \xi_1$ due to an incident plane wave traveling in the negative Z direction is shown in the bottom of Figure 13 The series converges rapidly enough to be conveniently evaluated by computer for values of $ka \leq 10$ The functions $S_{on}(-ika, \eta)$ and $R^{(3)}_{on}(-ika, i\xi_1)$ are oblate spheroidal wave functions

In order to determine the accuracy of the series solution for predicting surface pressures an experimental investigation of the diffraction of a plane wave by an oblate spheroid was conducted in an anechoic chamber The spheroid used in the test had a major diameter of 25 4 cm and a thickness of 8 08 cm which corresponds to a value $\xi_1 = 336$ The details of these measurements and a description of the experiment are given in reference 6 The spheroid was instrumented with seven surface pressure gauges on one side which were used to map the surface pressures in detail on both the sonified and shadow sides of the spheroid The incident wave was generated by a loud speaker placed at a distance of 3 5 m from the center of the spheroid Figure 14 shows a comparison between measured and predicted values of the ratio $|P_S/P_I|$ for several values of ka P_S is the surface pressure at a point on the spheroid and P_I is the free-field pressure at the same point in the absence of the spheroid At ka = 0 43 the pressure distribution around the spheroid is quite uniform varying only slightly from that in the incident wave At ka = 2 0 constructive interference more than doubles the pressure in the center of the top side of the spheroid, and a shadow begins to form on the bottom side At ka = 7 5 a large region of uniform pressure doubling extends on the top side of the surface and a more distinct and widespread shadow region characterized by pressures less than those in the incident wave begins to spread over the bottom side The overall agreement between theory and experiment is quite good over this range of ka values One can now proceed to apply the theory to calculating surface pressures and evaluating the scattering factor for a family of spheroidal shapes with confidence

The results of such a parameter study are shown in Figure 15 The parameter ξ_1 was varied from 0 to 1 producing a family of oblate spheroids The value $\xi_1 = 0$ corresponds to a flat thin disc whereas $\xi_1 = 1$ corresponds to a sphere The scattering factor measures the extent to which the finite difference approximation using measured surface pressures approximates the desired free-field pressure gradient at the center of the spheroid The smaller the magnitude of the scattering factor the better the approximation The criterion chosen to identify an optimum shape is $|\sigma| \leq 1$ over the largest possible range of the frequency parameter F It can be seen from the figure that for the four shapes shown the spheroid corresponding to $\xi_1 = 826$ is the best shape allowing measurement up to a value of the frequency parameter of 1 7 An extension of these optimum shape studies to bodies of more general shapes has been carried out in reference 7 using a finite element technique

WING SHIELDING OF AIRCRAFT ENGINE NOISE

One method for reducing the aircraft noise received by the airport community during landing approach and takeoff operations is to place the aircraft engine above the wing Observers on the ground may thereby be shielded from the direct radiation of some engine noise by the presence of the wing surface Three current engine over-the-wing aircraft configurations for which wing shielding may reduce community noise are shown in Figure 16 The QSRA is a NASA research aircraft The YC-14 is a STOL transport designed for military use by the Boeing Commercial Aircraft Company The jet engine exhaust close to the nozzle is then above the wing which tends to block off the downward radiation of jet noise from this part of the flow The VFW-614 has its two engines mounted completely above the wing on pylons The engine inlet is placed about over the mid-chord of the wing resulting, one would expect, in some shielding of ground observers from the forward radiated turbomachinery noise

An experiment to measure the potential shielding effects of an aircraft wing was reported in reference 8 The test model and test arrangement are shown in Figure 17 The model consisted of a simulated wing and flap system having a chord-length of about 0 37 meters The wing was very long in the span-wise direction, so as to simulate a two-dimensional arrangement The noise source was a broadband point source placed at two positions above the wing, at 20 percent and 50 percent chord Measurements of the diffracted sound field were made at increments of 10° from 20° to 160° below the wing as indicated in the sketch at the right of the figure The measurements, made along an arc of radius 0 66 meters were taken in one-third octave bands at frequencies from 800 to 10,000 Hz The measurements were made both with and without the wing in place and the results subtracted to obtain a change in sound pressure level, ΔSPL, due to the

presence of the wing in the field of the point source A positive ΔSPL indicates the decrease in the measured sound pressure level due to the shielding produced by the wing

Measurements of the wing shielding effect are shown in Figures 18 and 19 Figure 18 shows the difference in the shielding effect for the two different source positions at a frequency of 800 Hz The shielding effect for position II, which is at the mid-chord location, is symmetric about 90° Although there is a 5 dB shielding directly beneath the wing the maximum shielding effect, about 14 dB, occurs symmetrically ahead of and behind the overhead position at angles of 60° and 120° The shielding effect produced for the source at position I is unsymmetric about 90° The maximum shielding of about 13 dB is seen to occur at about 80° These directivity patterns come about as a result of the constructive and destructive interference which results from the superposition of waves diffracted around the leading and trailing edges of the airfoil The results of the figure show that achieving a desired shielding effect requires properly locating the wing relative to the noise source

Figure 19 shows measurements of the wing shielding effect for source position II for frequencies of 800, 1600, and 5,000 Hz In general, as the frequency increases the amount of shielding obtained below the wing increases As frequency increases, the shadow produced under the wing intensifies and for these experiments, produces nearly 25 dB of noise shielding directly below the wing at 5000 Hz

Shielding effects are therefore seen to depend both upon source frequency and source position Jet engine noise is both broadband in nature and is produced in a region which extends for considerable distance downstream of the jet nozzle It is evident, therefore, that designing for a optimum amount of engine noise shielding will require very careful design procedures The results of a flight test program to study shielding utilizing a delta wing fighter aircraft are reported in reference 9

DIFFRACTION BY AN AIRCRAFT FUSELAGE

It is of practical interest to know whether the diffraction of aircraft noise by the fuselage, wing and tail surfaces must be accounted for in aircraft noise prediction This is a difficult question to answer since it involves multiple distributed sources and complex geometries The possibility of such installation effects is suggested by the fact that the wavelengths of aircraft noise can be comparable to or smaller than the characteristic dimensions of the wing and fuselage surfaces A preliminary analytical study of the importance of scattering from the aircraft fuselage was conducted using a prolate spheroid with acoustic point sources on one major axis, reference 10 The geometry and coordinate system for this problem are shown in Figure 20

Several approaches for calculating the diffracted field of a point source near a prolate spheroid are available, see for example reference 1, including the series expansion method The method of geometric acoustics discussed earlier in the paper was selected because of the relative simplicity of the solution. Expressions for the sound field are obtained which can be quickly evaluated on a computer

The solution of the diffraction problem using geometric acoustics is given in Figure 21 A point source is at Q on the major axis of the prolate spheroid The incident velocity potential ϕ_1 at the point P_1 on the surface of the spheroid is given in equation 1 in which $\overline{QP_1}$ indicates the distance between points Q and P_1

The reflected field ϕ_r at a point P along a reflected ray is given by equation 2 in which θ is the angle of incidence, ρ_1 is the radius of curvature of the spheroid in the plane of incidence at P_1, and ρ_2 is the radius of curvature in the plane perpendicular to the plane of incidence and containing the normal to the spheroid at P_1 In order to calculate ϕ_r using equation 2 when Q and P are given, three computations must be made the reflection point P_1 must be located, the angle of incidence θ must be determined, and finally the two radii of curvature must be computed The details of this process are given in reference 10

To complete the calculation one must determine the diffracted field, ϕ_d The diffracted field is given in equation 3 in which ξ and η denote prolate spheroidal coordinates of points on the spheroid surface as indicated in Figure 4 of reference 10, and d is the interfocal distance. The functions $f_n(\eta)$ and $X_n(\alpha, \beta)$ are defined in reference 10 This formulation for the diffracted field is valid provided $ka(\frac{b}{a})^2 >> 1$ The complete solution for the acoustic velocity potential is ϕ_d in the shadow region and $\phi_1 + \phi_r + \phi_d$ in the sonified region

Sample calculations were made of the diffracted sound field for a spheroid which is the approximate size and shape of a commercial aircraft fuselage and for frequencies typical of aircraft noise Some results of these calculations are shown in Figure 22 The value ka = 1000 corresponds, for example, to a frequency of about 3500 Hz and a major axis of 30 meters The sketches show contours of equal sound pressure level on an imaginary observer plane below and parallel to the x, y plane, see Figure 20), at $\frac{z}{a} = 20$ The intersection of the z axis with this observer plane is the origin of the plots All sound pressure levels are normalized with respect to the SPL at this reference point

The sketch at the top of Figure 22 shows the circles of constant SPL produced by a simple stationary point source in the absence of the scattering body The sketch at the lower left shows the distortion produced in these contours by adding the spheroid The source is placed at a distance equal to 0 028a aft of the spheroid on the extension of the major axis The sketch at the lower right shows contours for the case of three correlated sources on the major axis of the spheroid The greater distortion of the equal SPL contours than in the case of one source is evident The complex patterns shown here resulting from diffraction by the fuselage are considered severe enough to warrant giving more attention to the possible effects of the scattering of aircraft noise by the airframe

A comparison of the geometric acoustic solution with other experimental and numerical results is shown in Figure 23 The integral equation solution method and the details of the experiment are discussed in the lecture entitled, "Acoustic Scattering from an Elliptic Body" by L Maestrello and A Bayliss in this lecture series The calculations are for a value ka = 164 which is considered sufficiently large for the geometrical theory to be applicable. The comparison with the more exact solution of Bayliss and the experimental data of Maestrello is seen to be quite acceptable except at small angles within the geometrical shadow region

TRAILING EDGE NOISE RADIATION

Trailing edge noise is a frequently occurring source of aircraft noise which has been found for instance on the STOL, VTOL, and CTOL configurations shown in Figure 24 Trailing edge noise is an aerodynamic noise source caused by the turbulent flow shed off the trailing edges of wings, flaps, or rotating blades The readjustment process which the flow makes as it transitions from being constrained by a surface to being a free shear flow results in the radiation of noise The turbulent flow may be either a boundary layer flow or a wall jet flow Thus, trailing edge noise has been encountered in connection with blown flaps used for the generation of powered lift, wings and flaps, from which it is a source of airframe noise, and rotating blades for which it is a broadband noise source

The currently accepted theory of trailing edge noise generation is shown in Figure 25, see reference 11 The airfoil is idealized as a semi-infinite flat rigid surface in a uniform stream, U_0, parallel to the plate A boundary layer flow develops over the upper and lower surfaces A typical turbulent eddy in the flow field, with vorticity of $\overline{\omega}$, travels downstream parallel to the plate at a velocity $\overline{V}$ As this eddy passes across the trailing edge of the plate a counterrotating eddy is generated with a circulation $\overline{\Omega}$ which then proceeds to travel downstream at the velocity $\overline{W}$ The vorticity $\overline{\Omega}$ of the induced eddy is determined by the condition imposed upon the flow field at the trailing edge of the plate Two extreme conditions have been considered a full Kutta condition, which stipulates that there will be no pressure difference across the plate at the trailing edge and the contrary condition in which no vorticity at all is shed into the wake in which case the pressure difference at the trailing edge of the plate becomes infinite

The partial differential equation governing the generation and propagation of sound by turbulent trailing edge eddies is shown in the center of Figure 25 The equation consists of a convective wave operator which describes the propagation of sound through the externally moving medium and an inhomogeneous term on the right hand side of the equation which is responsible for the generation of sound by the eddies The two vectors $\overline{\omega} \times \overline{V}$ and $\overline{\Omega} \times \overline{W}$ each lie in the plane of the sketch normal to the plate These vectors play the role of externally applied body forces in the turbulent fluid surrounding the trailing edge which act normal to the trailing edge Thus, the trailing edge noise source may be interpreted as a distribution of dipoles in the wake whose strength is related to the vorticity in the fluid and the convection speed of the turbulent eddies In the formulation of this theory it was found to be convenient to use as the principal acoustic variable the stagnation enthalpy B in the flow field which is related to the far-field acoustic pressure as indicated in the equation at the bottom of the figure in which $\overline{M}_0$ is the component of the free stream Mach number in the direction of the observer On the plate the normal derivative of B vanishes

Trailing edge noise is generated then by dipoles located near the trailing edge of the plate and normal to the plane of the plate. Because of the presence of the plate the directivity pattern of a trailing edge dipole will be different than that of a free-field dipole as a result of acoustic diffraction phenomenon The directivity of a trailing edge dipole is shown in Figure 26 The angles α and θ defining the observer position are shown in the sketch The mean square pressure in the acoustic far field is proportional to $\sin \alpha \sin^2 \frac{\theta}{2}$ Several cross sections through the radiation pattern of such a baffled dipole are shown in the sketches at the bottom of the figure This dipole has its maximum radiation amplitude in the plane of the plate in contrast to the radiation from the free-field dipole which achieves its maximum along the axis of the applied force and has no radiation perpendicular to the force axis The theory predicts that the amplitude of the mean square pressure depends upon the boundary conditions imposed at the trailing edge

A comparison between measured and predicted directivity patterns of trailing edge noise, taken from reference 12, is shown in Figure 27 The trailing edge noise was produced by placing a thin plate in a jet exhaust as indicated by the sketch in the middle of the figure Measurements of the radiated noise were then taken in narrow bands at the six frequencies between 100 and 3,000 Hz Note that the dB levels on the upper and lower halves of the figure are different There is a consistent and appreciable decrease in amplitude with increasing frequency At any frequency there is a clear tendency for the radiated noise to peak in the upstream direction, as predicted by the theory. This type of evidence supports the general correctness of the theoretical prediction of trailing edge noise radiation The additional diffraction which may be expected from the leading edge of a plate of finite length is discussed in references 12 and 13

CONCLUDING REMARKS

This paper has provided an introduction to the concepts and methods of diffraction theory and has presented several examples of diffraction phenomena arising in the study of aircraft noise It has been shown how the diffraction theory was used to select the shape of a microphone so as to extend its usefulness over the widest possible frequency range Experiments on wing shielding of engine noise show the potential for considerable reduction of the community noise through proper engine placement The scattering of sound from an aircraft fuselage was studied using a geometrical theory of diffraction Severe distortions of equal sound pressure level contours were observed suggesting that the scattering of noise from the airframe deserves more attention Experiments and theory on trailing edge noise indicate that the diffracting effect of the wing explains the unusual cardioid radiation pattern of this noise source The need for more powerful theoretical methods to calculate diffraction phenomena for complex shapes and broadband distributed sources is clear

REFERENCES

1 Asvestas, J S , Bowman, J J., Christiansen, P. L., Einarsson, O , Kleinman, R E , Sengupta, D L , Senior, T B A , Sleator, F B , Uslenghi, P L E , Zitron, N R Electromagnetic and Acoustic Scattering by Simple Shapes North-Holland Publishing Company, Wiley Interscience Division, John Wiley & Sonc, Inc - New York, 1969

2 Bouwkamp, C J Reports on Progress in Physics (Diffraction Theory), Vol XVII, 1954, published by The Physical Society, London

3 Morse, Philip M , Feshbach, Herman Methods of Theoretical Physics Part II, Chapter 11, McGraw-Hill Book Company, Inc , 1953

4 Morse, Philip M , Ingard, K Uno Theoretical Acoustics Chapter 8, McGraw-Hill Book Company, 1968

5 Lewis, Robert M , Keller, Joseph B Asymptotic Methods for Partial Differential Equations The Reduced Wave Equation and Maxwell's Equation. Research Report No EM-194, New York University, Courant Institute of Mathematical Sciences, January 1964, Contract No AF 19(604)5238, Project No 5635, Task No 563502

6 Maciulaitis, Algirdas, Seiner, John M , Norum, Thomas D Sound Scattering by Rigid Oblate Spheroids, with Implication to Pressure Gradient Microphones NASA TN D-8140, May 1976

7 Norum, Thomas D , Seiner, John M Shape Optimization of Pressure Gradient Microphones NASA TM 78632, December 1977

8 Sears, Frederick M The Acoustic Shielding of Noise by a Jet Wing Submitted in partial fulfillment of the requirements for the degrees of Bachelor of Science and Master of Science at the Massachusetts Institute of Technology, May 1975

9 Jeffery, R W , Holbeche, T A An Experimental Investigation of Noise-Shielding Effects for a Delta-Winged Aircraft in Flight, Wind Tunnel and Anechoic Room Tech Memo AERO 1621, Royal Aircraft Establishment, February 1975

10 Padula, S L , Liu, C H Acoustic Scattering of Point Sources by a Moving Prolate Spheroid AIAA 4th Aeroacoustics Conference, Atlanta, Georgia, October 3-5, 1977, Paper No 77-1326

11 Howe, M S A Review of the Theory of Trailing Edge Noise NASA Contractor Report 3021, June 1978

12 Hayden, Richard E , Fox, Herbert L , Chanaud, Robert C Some Factors Influencing Radiation of Sound from Flow Interaction with Edges of Finite Surfaces Bolt Beranek & Newman Report No 2797, July 1976

13 Tam, Christopher K W , Yu, J C Aeroacoustics STOL Noise, Airframe and Airfoil Noise (Trailing Edge Noise) Volume 45, Progress in Astronautics and Aeronautics, 1976

ACKNOWLEDGEMENT

The authors would like to acknowledge the assistance of Ms Jean Mason with various calculations presented in this paper

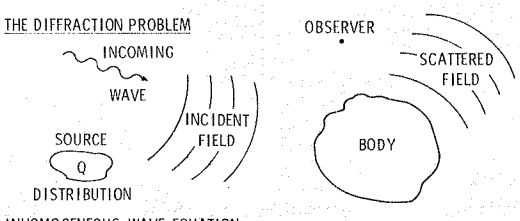

INHOMOGENEOUS WAVE EQUATION

$$\frac{1}{c^2}\cdot\frac{\partial^2\varphi}{\partial t^2} - \nabla^2\varphi = Q$$

φ ACOUSTIC VELOCITY POTENTIAL — $p = \rho_0 \frac{\partial \varphi}{\partial t}$ ACOUSTIC PRESSURE

c AMBIENT SPEED OF SOUND — $\bar{u} = -\nabla\varphi$ ACOUSTIC VELOCITY VECTOR

Figure 1 - Basic Equations of Acoustic Diffraction Theory - Field Equation

SURFACE BOUNDARY CONDITION

$\rho_0 c u_n = \nu p$; ν = SPECIFIC SURFACE ADMITTANCE.

$\nabla\varphi\cdot\bar{n} + \frac{\nu}{c}\frac{\partial\varphi}{\partial t} = 0$ ON THE BODY SURFACE.

RADIATION CONDITION

OUTGOING WAVES AT LARGE DISTANCES

$\frac{\partial\varphi}{\partial r} + \frac{1}{c}\frac{\partial\varphi}{\partial t} \to 0$ OR $p \approx \rho_0 c\, u_r$ AS $r \to \infty$.

EDGE CONDITION

NO ENERGY IS GENERATED AT SHARP EDGES.

$\iiint_{\text{FINITE REGION}} [\nabla\varphi\cdot\nabla\varphi]\, dv$ IS FINITE.

Figure 2 - Basic Equations of Acoustic Diffraction Theory - Auxillary Conditions

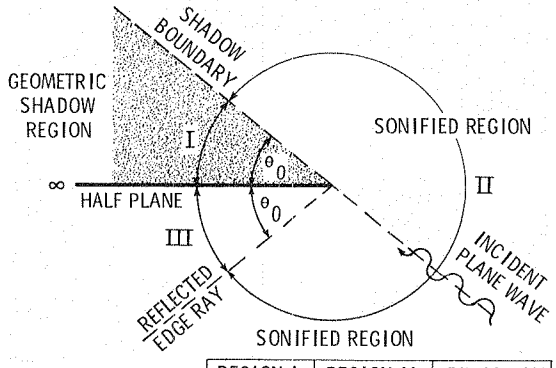

	REGION I	REGION II	REGION III
	SHADOW	SONIFIED	
DIFFRACTED WAVE	✓	✓	✓
INCIDENT WAVE	X	✓	✓
REFLECTED WAVE	X	X	✓

Figure 3 - Plane Wave Diffraction by a Half Plane-Interpretation of Solution

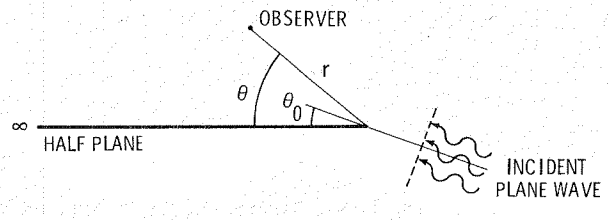

$$p = \frac{e^{-i\pi/4}}{\sqrt{\pi}}\left\{ e^{ikr\,\mathrm{Cos}(\theta-\theta_0)}\,\Phi\left(\sqrt{2kr}\,\sin\tfrac{1}{2}(\theta-\theta_0)\right) + e^{ikr\,\mathrm{Cos}(\theta+\theta_0)}\cdot\Phi\left(-\sqrt{2kr}\,\sin\tfrac{1}{2}(\theta+\theta_0)\right)\right\}$$

$$\Phi(x) = \int_{-\infty}^{x} e^{it^2}\,dt = \text{FRESNEL INTEGRAL}$$

Figure 4 - Plane Wave Diffraction by a Half Plane-Exact Mathematical Solution

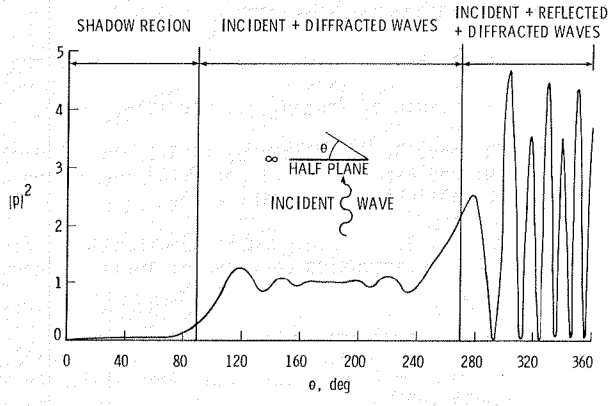

Figure 5 - Mean Square Pressure in the Sound Field for Plane Wave Diffraction by a Half Plane-Normal Incidence: kr = 6π

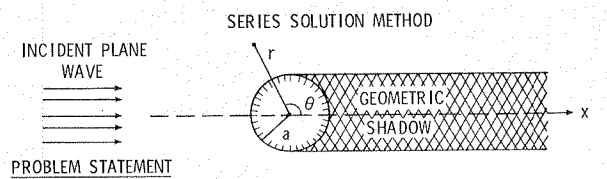

PROBLEM STATEMENT

$\nabla^2\varphi + k^2\varphi = 0$; TIME FACTOR $e^{-i\omega t}$

φ = PLANE WAVE + OUTGOING WAVES ; $\left.\frac{\partial\varphi}{\partial r}\right|_{r=a} = 0$

SOLUTION METHOD

$\varphi = \varphi_i + \varphi_s$

$$\varphi_i = e^{ikx} = e^{ikr\,\mathrm{Cos}\,\theta} = \sum_{n=0}^{\infty} i^n\,\varepsilon_n\,J_n(kr)\,\mathrm{Cos}\,n\theta$$

$$\varphi_s = \sum_{n=0}^{\infty} i^n\,\varepsilon_n\,A_n\,H_n^{(1)}(kr)\,\mathrm{Cos}\,n\theta$$

Figure 6 - Diffraction of a Plane Wave by a Cylinder - Series Solution Method

SOLUTION METHOD

$$\varphi = \sum_{n=0}^{\infty} i^n \varepsilon_n \left[J_n(kr) + A_n H_n^{(1)}(kr) \right] \cos n\theta$$

$$\left.\frac{\partial \varphi}{\partial r}\right|_{r=a} = 0 = \sum_{n=0}^{\infty} i^n \varepsilon_n \left[J_n'(ka) + A_n H_n^{(1)\prime}(ka) \right] \cos n\theta$$

$$\therefore A_n = -J_n'(ka)/H_n^{(1)\prime}(ka)$$

$$P = P_i + P_s = -i k \rho_0 c \varphi \qquad ; \qquad \bar{u} = \bar{u}_i + \bar{u}_s = -\nabla \varphi$$

ACOUSTIC FAR FIELD

FOR $kr \to \infty$: $P_s \approx \rho_0 c (u_r)_s \approx \rho_0 c \sqrt{\frac{k}{r}} e^{i(kr + \frac{\pi}{4})} P(ka, \theta)$

$$P(ka, \theta) = \sqrt{\frac{2}{\pi}} \sum_{n=0}^{\infty} \varepsilon_n \frac{J_n'(ka)}{H_n^{(1)\prime}(ka)} \cos n\theta$$

Figure 7 - Diffraction of a Plane Wave by a Cylinder - Far-Field Acoustic Solution

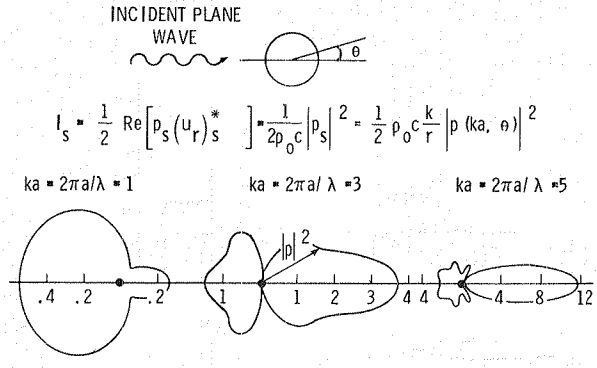

Figure 8 - Scattered Intensity for Diffraction of a Plane Wave by a Cylinder

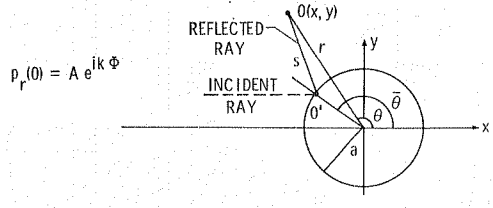

Figure 9 - Plane Wave Diffraction by a Circular Cylinder-Geometric Theory: Reflected Waves

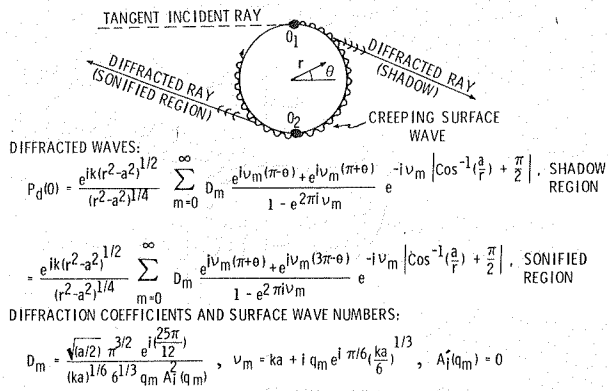

Figure 10 - Plane Wave Diffraction by a Circular Cylinder-Geometric Theory: Diffracted Waves

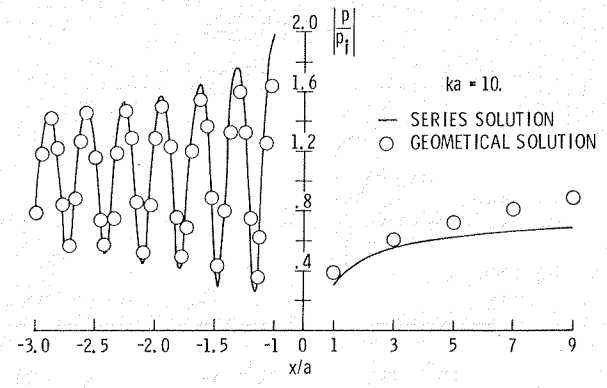

Figure 11 - Comparison Between Series Solution and Geometric Acoustics

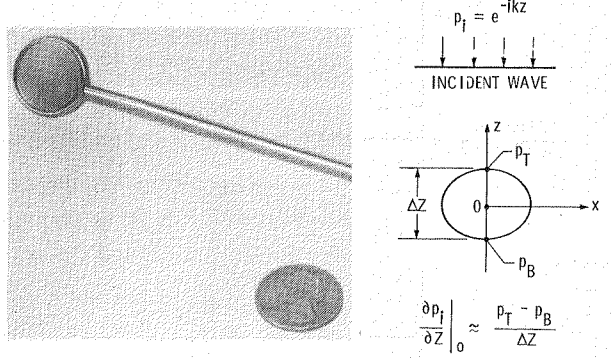

Figure 12 - Pressure Gradient Microphone - Appearance and Function

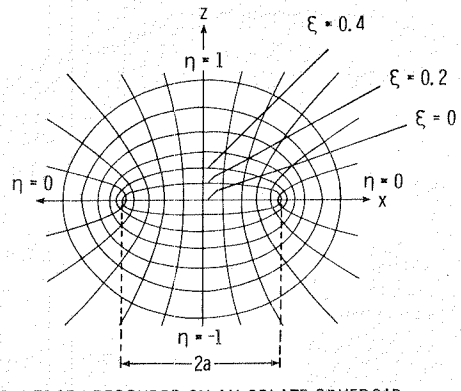

SURFACE PRESSURES ON AN OBLATE SPHEROID

$$\frac{p_s(\eta, \xi_1)}{p_i} = \frac{2}{ka\left(1 + \xi_1^2\right)} \sum_{n=0}^{\infty} i^n \frac{S_{on}(-ika, -1) S_{on}(-ika, \eta)}{N_{on}(-ika) R_{on}^{(3)'}(-ika, i\xi_1)}$$

Figure 13 - Oblate Spheroidal Coordinates

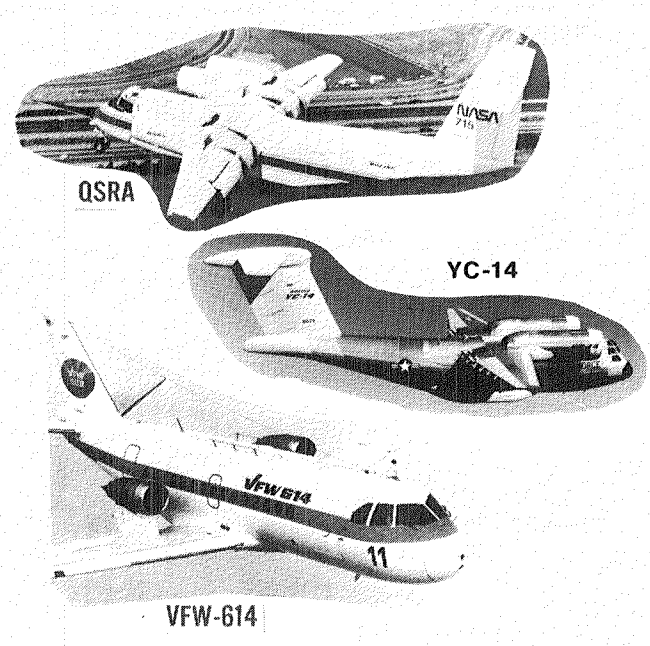

Figure 16 - Engine Over the Wing Aircraft Configurations

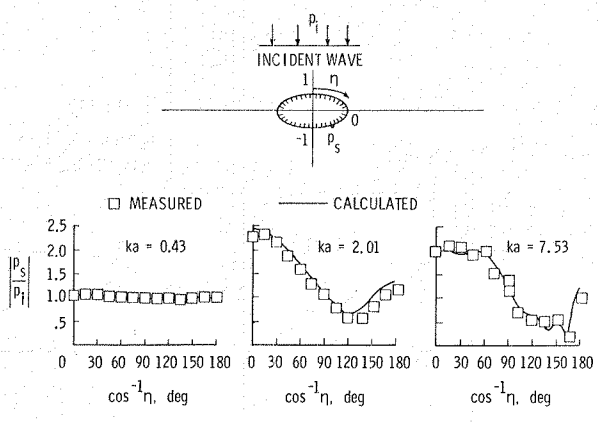

Figure 14 - Comparison of Measured and Calculated Surface Pressures

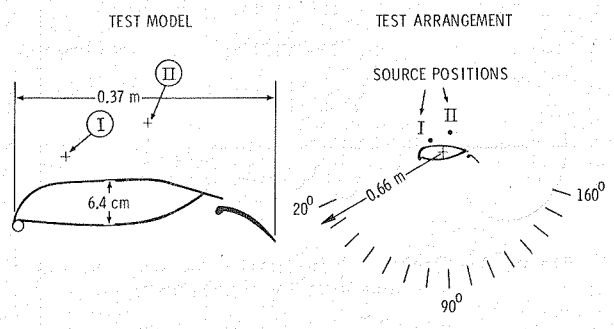

Figure 17 - Wing Shielding Experiment

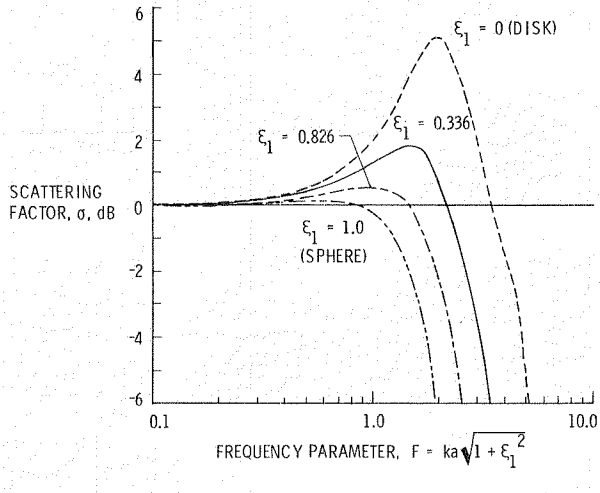

Figure 15 - Variation of Scattering Factor with Frequency Parameter

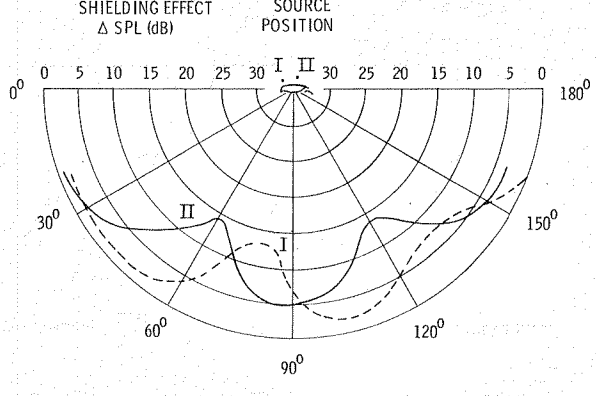

Figure 18 - Measured Wing Shielding Effect Chord/Wave length = 0.85, f = 800 Hz

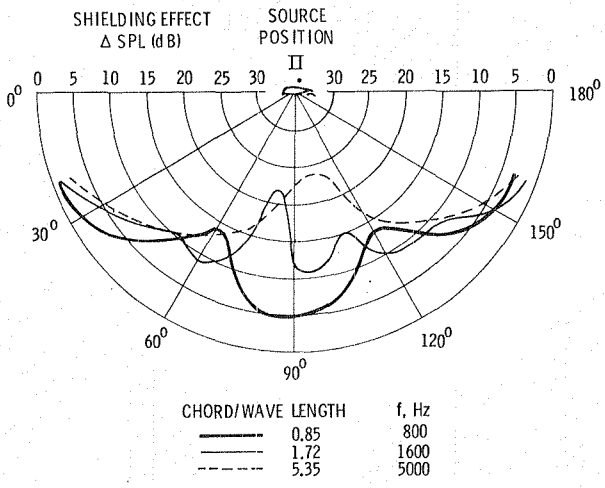

Figure 19 - Measured Wing Shielding Effect

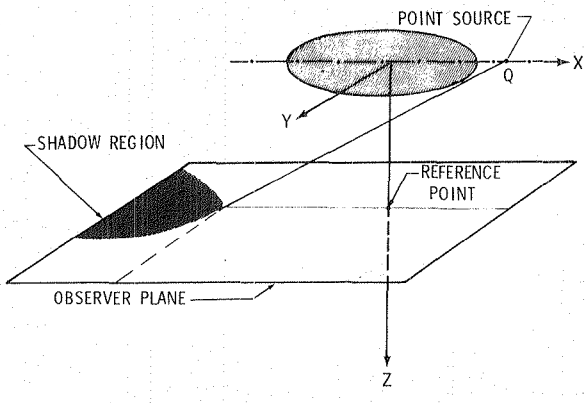

Figure 20 - Acoustic Scattering of Point Source by an Aircraft Fuselage

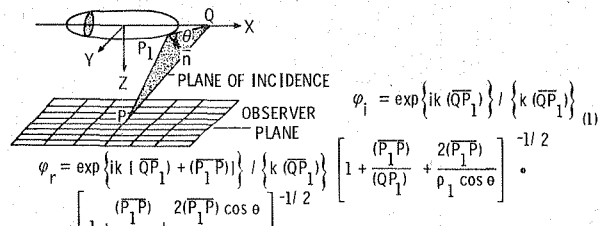

$$\varphi_i = \exp\left\{ik\,(\overline{QP}_1)\right\} / \left\{k\,(\overline{QP}_1)\right\} \quad (1)$$

$$\varphi_r = \exp\left\{ik\,[\,(\overline{QP}_1) + (\overline{P_1P})]\right\} / \left\{k\,(\overline{QP}_1)\right\} \left[1 + \frac{(\overline{P_1P})}{(\overline{QP}_1)} + \frac{2(\overline{P_1P})}{\rho_1 \cos\theta}\right]^{-1/2} \cdot \left[1 + \frac{(\overline{P_1P})}{(QP)} + \frac{2(\overline{P_1P})\cos\theta}{\rho_2}\right]^{-1/2} \quad (2)$$

$$\varphi_d = \frac{2^{3/2} \exp\left\{\frac{i\pi}{12}\right\} \left[\varepsilon_1\sqrt{\varepsilon_1^2 - 1}\right]^{1/6}}{\pi^{1/2}\,(2kd)^{7/6}} \cdot \frac{\exp\left[(ikd/2\varepsilon_0)\sqrt{(\varepsilon_0^2 - 1)(\varepsilon_0^2 - \varepsilon_1^2)}\right]}{\left[(\varepsilon_0^2 - \varepsilon_1^2)(\varepsilon_0^2 - 1)(\varepsilon^2 - 1)(1 - \eta^2)\right]^{1/4}} \cdot \sum_{n=0}^{\infty} \frac{\tilde{f}_n(\eta_2) - i\tilde{f}_n(\eta_3)}{\beta_n\,[\,Ai(-\beta_n)]^2\,[\,1 + \exp\left\{2\tilde{X}_n(1, -1)\right\}\,]} \quad (3)$$

Figure 21 - Geometrical Theory of Scattering by a Prolate Spheroid

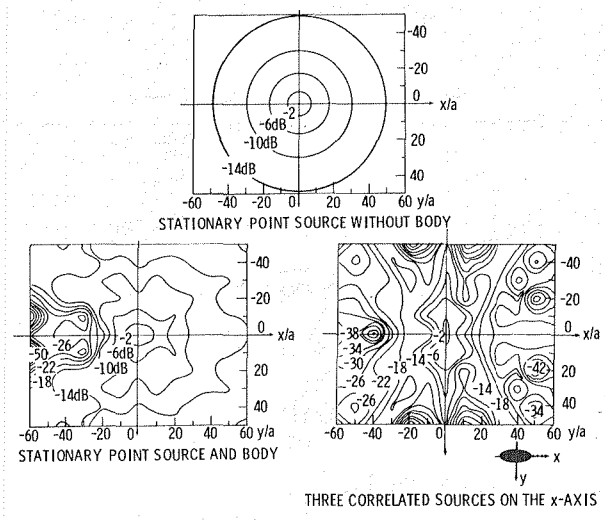

Figure 22 - Sound Pressure Level Contours on Observer Plane
ka = 1000, b/a = 0.14, z/a = 20

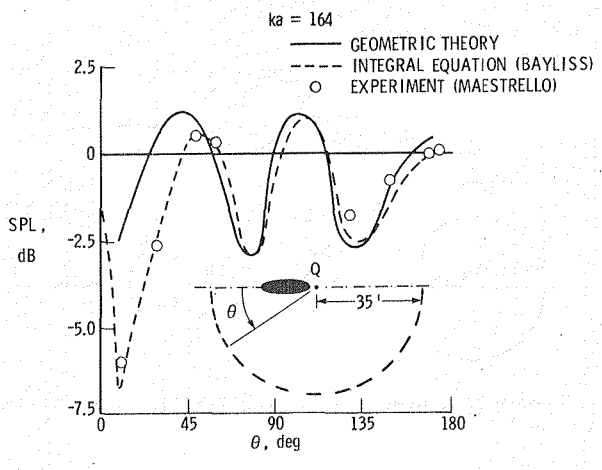

Figure 23 - Validation of Computational Method
ka = 164

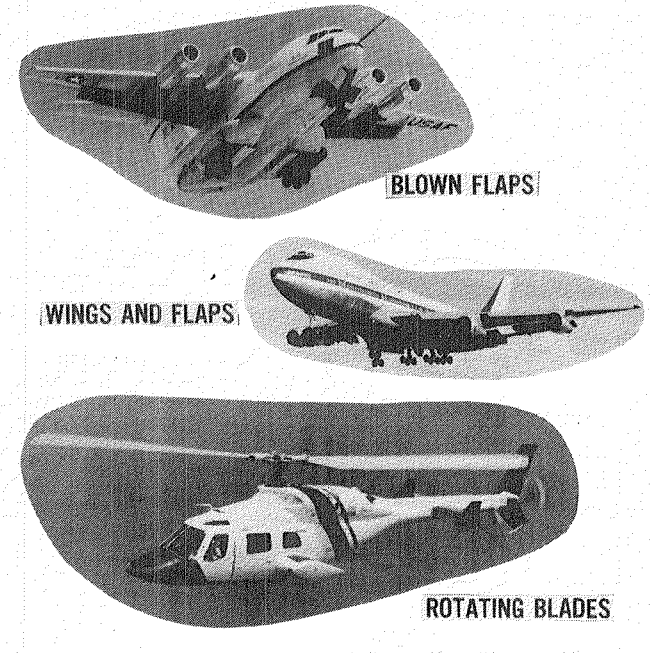

Figure 24 - Aircraft Trailing Edge Noise Sources

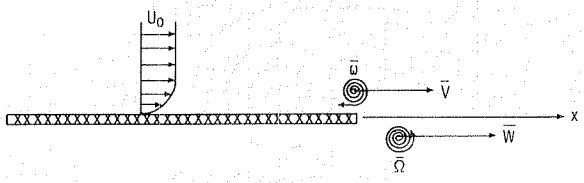

$$\left[\frac{1}{c^2}\left(\frac{\partial}{\partial t} + U_0\frac{\partial}{\partial x}\right)^2 - \nabla^2\right] B = \text{div}\,(\bar{\omega}\times\bar{V}) + \text{div}\,(\bar{\Omega}\times\bar{W})$$

CONVECTED WAVE OPERATOR — EDGE DIPOLE DISTRIBUTION

$$B = h + \frac{1}{2}\bar{v}\cdot\bar{v} \sim (1+\bar{M}_0)\frac{p}{\rho_0} \quad \text{IN THE FAR FIELD}$$

Figure 25 - Howe Trailing Edge Noise Theory

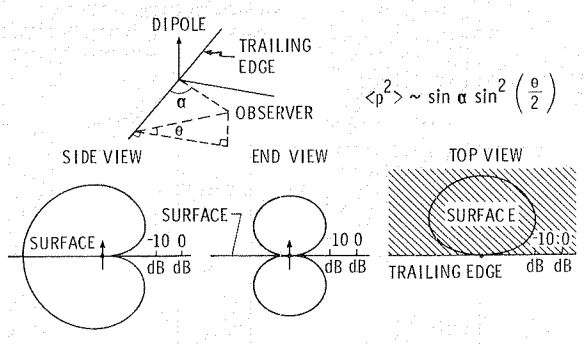

Figure 26 - Directivity of a Trailing Edge Dipole

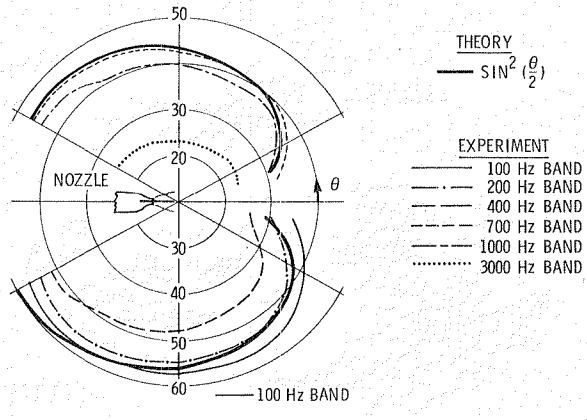

Figure 27 - Measured Directivity of Trailing Edge Noise

End of Document